Available online at www.sciencedirect.com
ScienceDirect
Journal of Electroanalytical Chemistry 599 (2007) 367–375
Journal of Electroanalytical Chemistry
www.elsevier.com/locate/jelechem

Analysis of adsorption of phospholipids at the 1,2-dichloroethane/water interface by electrochemical impedance spectroscopy: A study of the effect of the saturated alkyl chain

M.C. Martins [a], C.M. Pereira [a,*], H.A. Santos [a,1], R. Dabirian [a,2], F. Silva [a], V. Garcia-Morales [b], J.A. Manzanares [b]

[a] *Departamento de Química da Faculdade de Ciências da Universidade do Porto, Rua do Campo Alegre 687, P-4169-007 Porto, Portugal*
[b] *Departament de Termodinàmica, Universitat de València, C/Dr. Moliner 50, E-46100 Burjassot, Spain*

Received 7 December 2005; received in revised form 9 June 2006; accepted 20 July 2006
Available online 8 September 2006

Abstract

The adsorption behaviour of a series of phosphatidylcholines (PCs) with saturated carbon chains of different length (DLPC, DPPC, DSPC, DAPC, and DBPC) at the electrified 1,2-dichloroethane/water interface was studied by measuring electrochemical impedance spectroscopy at the polarized interface. Two different trends in the interfacial capacitance were observed for any of the PCs the capacity dependence on the applied potential: strong adsorption occurs at negative potential with a marked decrease of $C(E)$; increase of capacity is observed at positive potentials. It is demonstrated that the interfacial lipid adsorption was dependent on phospholipid concentration, applied potential, and phospholipid chain length. The potential and concentration dependence of the interfacial capacitance in the presence of these phospholipids were successfully described by a model based on the solution of the Poisson–Boltzmann equation in the interfacial region.

Keywords: Liquid–liquid interface; Phospholipid adsorption; Electrochemical impedance spectroscopy; Interfacial capacitance

1. Introduction

The adsorption of phospholipids have received extensive attention particularly at the air–water and liquid–liquid interfaces.

Pethica and co-workers [1] measured the surface pressure isotherms for a series of insoluble (distearoyl phosphatidylcholine—DSPC and dioleoyl phosphatidylcholine—DOPC) at the *n*-heptane/water interface using a Langmuir trough. These authors concluded that DSPC forms monolayers which were affected by the concentration of the aqueous electrolyte (NaCl which concentration is varied between 0.1 and 0.01 M) and by the pH (between 2 and 5). Later on, Pethica et al. [2] extended this study to an homologous series of 1,2-diacyl-PC (from C14 to C22) and compared the results with di-C_{14}-cephalin. They concluded that the chains of the phospholipids were fully flexible at low coverage as the isotherms were independent of chain length. This conclusion was supported by the absence of any phase transition between 5 and 25 °C as it was observed previously for air/water interface [3]. By contrast on the high coverage region the experimental results by

* Corresponding author. Tel.: +351 226082941; fax: +351 226082959.
E-mail address: cmpereir@fc.up.pt (C.M. Pereira).
[1] Present address: Department of Chemical Technology, Laboratory of Physical Chemistry and Electrochemistry, Helsinki University of Technology, Finland.
[2] Present address: Department of Physical Organic Chemistry Debye Research Institute Utrecht University, H.R. Kruytgebouw, W808 Padualaan 8, 3584 CH Utrecht, The Netherlands.

0022-0728/$ - see front matter © 2006 Elsevier B.V. All rights reserved.
doi:10.1016/j.jelechem.2006.07.022

Mingins et al. [4] showed the presence of phase transitions for phosphatidylcholines (PCs) with chains having more than 16 carbon atoms. Moreover, the temperature dependence was found to be greater for the longer chain PCs.

The adsorption of PCs at a deuterated water/carbon tetrachloride interface (22 °C) [5] shows the formation of highly packed layers for dilauryl-PC (DLPC) (50 ± 8 Å^2/molecule) and dimyristoyl-PC (DMPC) (70 ± 15 Å^2/molecule) and expanded layers for dipalmitoyl-PC (DPPC) and DSPC (100 Å^2/molecule). The state of organization of those PCs seems to vary little with the organic phase since these values are very similar to those obtained for the *n*-heptane/water interface (20 °C) [4] and 1,2-dichloroethane (1,2-DCE)/water [6] interface (20 °C).

Electrical phenomena at the surface of lipidic membranes are fundamental to understand the mechanism of membrane transport of ions and molecules [7]. The use of polarized ITIES is probably one of the best ways to study adsorption under the control of the potential across a lipid layer and the properties of adsorbed layers of phosphatidylcholines. The first studies of phospholipid adsorption at electrified liquid–liquid interface were presented by Watanabe et al. [8,9]. These authors measured the electrocapillary curves for the electrified interface formed between methylisobutylketone and water and were able to describe and characterize the adsorption of phospholipids. Some interesting results were described namely the interaction between the lipids and the cations in the aqueous phase and the effect of pH on the surface tension curves. However, the fact that Watanabe and co-workers used very small amounts of tetrabutylammonium chloride (50 μM) [9] in the organic phase or no supporting electrolyte [8], introduced some difficulties in the interpretation of the results. Later on, Girault and Schiffrin [10] studied the adsorption of PCs and phosphatidylethanolamines (PEs) from egg yolk at the electrified 1,2-DCE/water interface. The results showed a strong dependency of the surface tension on the interfacial potential. Furthermore, by analysing the electrocapillarity curves, two different trends could be observed: at more positive potentials the surface tension remained unchanged when varying the potential, and at more negative potential there was a strong increase of surface tension with the potential indicating a strong adsorption.

Kakiuchi and co-workers studied the adsorption of PCs [11,12] PE [13] and phosphatidylserine [14] at the nitrobenzene/water interface measuring interfacial capacitance and interfacial tension [15,16]. These authors extracted the Gibbs energy for the adsorption of the phospholipids at the liquid–liquid interface and concluded that the weak interactions between the lipid molecules are probably caused by the penetration of solvent molecules within the adsorbed lipid chains.

Wandlowski et al. [17,18] measured $C(E)$ curves for the adsorption of DLPC, DMPC and DPPC at the nitrobenzene/water interface from which the surface tension curves where calculated using an inner layer correction prior to the data integration. Although the adsorption Gibbs energy (−35.7 to −37.9 kJ/mol) is similar to that reported by Kakiuchi and co-workers (between −31 and −37 kJ/mol) a contrasting conclusion was reached concerning the net interactions of the adsorbed phospholipids as judged by the sign of the interaction parameter of the Frumkim isotherm: Wandlowski et al. obtained a negative value of the interaction parameter suggesting weak repulsive interactions between the adsorbed molecules while Kakiuchi et al. [11,16] proposed the existence of weak attractive interactions.

The interaction between aqueous cations and adsorbed phospholipids at the ITIES have also received particular attention by several authors, showing that cation complexation can be evaluated and can be responsible for the behaviour observed at more positive potentials [16,19–21].

Grandell et al. [6,22] reported a new electrochemical system coupled with a Langmuir trough, which allows the simultaneous control of surface pressure and the potential drop across the adsorbed layer. These authors presented adsorption isotherms for DPPC and DSPC at the air/water and 1,2-DCE/water interfaces and showed that in contrast to the air–water system, the latter isotherms did not display well-defined plateau regions or phase transitions. They interpreted the different behaviour as probably due to a high mobility in the surface of small size 1,2-DCE molecules. They further concluded that at positive potentials the adsorption of these lipids at 1,2-DCE/water was weak while at negative potentials rather stable monolayers were obtained. Apparently the compressibility of the adsorbed layer when the lipid molecules are compressed by a mechanic barrier is much higher than when it is obtained through continuous compression by successive addition of lipid aliquots [23]. However, these two modes cannot be compared as the monolayer collapse occurs with lipids at different orientations [23,24]. The introduction of a gelled phase allow the preparation and deposition of Langmuir–Blodgett films of phospholipids at a liquid–gel interface [25–27] and study the effect of film organization on capacitance and transport properties of the films.

In the present work, the adsorption of PCs with different chain length (C12, C16, C18, C20 and C22) and the effect of experimental parameters on the adsorption process were studied at the *electrified 1,2-DCE/water interface*. Impedance spectroscopy has been shown to be a simple and effective method to study the adsorption of phospholipids [11,13] therefore, impedance spectroscopy (EIS) was used to follow the adsorption phenomena of these lipids at the electrified liquid–liquid interface. The data were also fitted to the Frumkin adsorption model, which will be discussed according to the current knowledge on the structure and stability of adsorbed phospholipid monolayers at liquid–liquid interfaces.

Although similar to other systems reported in the literature our studies extend the potential window available thus allowing to observe the capacitance behavior at the more positive potentials, namely the drop in capacitance for

DAPC and DBPC at moderate concentrations. Furthermore for other lipids capacitance at higher concentration were obtained showing a decrease in capacitance apparently not reported before. Within the same potential region the results extend the effect of chain length to existing published data. The results allow to suggest that the current view of phospholipids adsorption on liquid/liquid surfaces is incomplete deserving further attention.

A theoretical model based in the solution of the Poisson–Boltzmann equation for the interfacial system coupling the bulk phases with a dielectric layer is used to interpret the data obtained. On previous works, similar models have been proven very useful for describing the polyelectrolyte multilayers adsorption at liquid–liquid interfaces and to gain structural insight of interfacial nanostructures deposited at a liquid–liquid interface [28,29].

2. Theory

The interfacial system is depicted in Fig. 1. The hydrocarbon region of the phospholipids is assumed to have a variable width depending both on the chain length, orientation and the phospholipid concentration. The capacitance C of the interfacial nanostructure is defined as [28]

$$C \equiv \frac{\partial Q}{\partial \Delta_{\mathrm{o}}^{\mathrm{w}}\phi} \tag{1}$$

where Q is the charge density separated across the ITIES and $\Delta_{\mathrm{o}}^{\mathrm{w}}\phi \equiv \phi_{\mathrm{w}}^{\mathrm{b}} - \phi_{\mathrm{o}}^{\mathrm{b}}$ is the Galvani potential difference between the bulk aqueous and organic phases. The interface is described by using a one-dimensional model in which the ITIES is located at the plane $x = 0$, the organic phase occupies the region $x < 0$, and the aqueous solution the region $x > 0$. The organic and aqueous bulk phases (i.e., the regions outside the electrical double layer at the ITIES) have molar concentrations of their respective 1:1 base electrolytes $c_{\mathrm{o}}^{\mathrm{b}}$ and $c_{\mathrm{w}}^{\mathrm{b}}$, and relative electrical permittivities ε_{o} and ε_{w}, respectively.

The hydrocarbon chains of the phospholipids occupy the region $-d_{\mathrm{hc}} < x < 0$, which is characterized by a relative permittivity $\varepsilon_{\mathrm{hc}}$. The different permittivity of the hydrocarbon region and the organic phase implies that a chemical partition coefficient K_{hc} needs to be included when describing the spatial distribution of the organic base electrolyte, and hence its effective concentration in the hydrocarbon region is $c_{\mathrm{hc}}^{\mathrm{b}} = K_{\mathrm{hc}} c_{\mathrm{o}}^{\mathrm{b}}$. The charge at the interface $x = 0$ is modelled as a plane distribution with electrical charge density σ_0 or, in dimensionless units, $\alpha \equiv A\sigma_0/e$, where e is the elementary charge and A is the mean molecular area of the phospholipids in the monolayer.

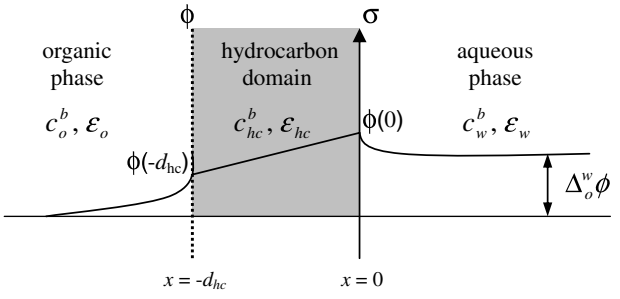

Fig. 1. Schematic representation of the electric potential distribution (solid line) in the interfacial system.

The electric potential distribution in region i (i = o, hc, w) is described by the Poisson–Boltzmann equation [30]

$$\frac{\mathrm{d}^2\varphi}{\mathrm{d}x^2} = \kappa_i^2 \sinh\left(\varphi - \varphi_i^{\mathrm{b}}\right) \tag{2}$$

where $\varphi \equiv F\left(\phi - \phi_{\mathrm{o}}^{\mathrm{b}}\right)/RT$ is the dimensionless electric potential, $\varphi_{\mathrm{hc}}^{\mathrm{b}} \equiv \varphi_{\mathrm{o}}^{\mathrm{b}} = 0$,

$$\kappa_i \equiv \left(\frac{2F^2 c_i^{\mathrm{b}}}{\varepsilon_i \varepsilon_0 RT}\right)^{1/2} \tag{3}$$

is the Debye parameter in region i, and ε_0 is the vacuum electrical permittivity. Multiplying Eq. (2) by $2\mathrm{d}\varphi/\mathrm{d}x$, it can be integrated to

$$\frac{\mathrm{d}\varphi}{\mathrm{d}x} = \pm\left[\kappa_i^2 \sinh^2\left(\frac{\varphi - \varphi_i^{\mathrm{b}}}{2}\right) + a_i\right]^{1/2} \tag{4}$$

where the plus and minus signs apply in the domains $x < 0$ and $x > 0$, respectively, and a_i is an integration constant. In the bulk phases the integration constant vanishes because $\mathrm{d}\varphi/\mathrm{d}x$ also does.

The constant a_{hc} as well as the potentials $\varphi(-d_{\mathrm{hc}})$ and $\varphi(0)$ are unknowns which have to be determined from the boundary conditions for the electric displacement

$$\varepsilon_{\mathrm{o}} \left.\frac{\mathrm{d}\varphi}{\mathrm{d}x}\right|_{x=-d_{\mathrm{hc}}^-} = \varepsilon_{\mathrm{hc}} \left.\frac{\mathrm{d}\varphi}{\mathrm{d}x}\right|_{x=-d_{\mathrm{hc}}^+} \tag{5a}$$

$$\varepsilon_{\mathrm{hc}} \left.\frac{\mathrm{d}\varphi}{\mathrm{d}x}\right|_{x=0^-} = \varepsilon_{\mathrm{w}} \left.\frac{\mathrm{d}\varphi}{\mathrm{d}x}\right|_{x=0^+} + \frac{F\sigma_0}{\varepsilon_0 RT} \tag{5b}$$

and the integral of Eq. (4) over the hydrocarbon region

$$\int_{\varphi(-d_{\mathrm{hc}})}^{\varphi(0)} \frac{\mathrm{d}\varphi}{\left[\kappa_{\mathrm{hc}}^2 \sinh^2(\varphi/2) + a_{\mathrm{hc}}\right]^{1/2}} = d_{\mathrm{hc}} \tag{6}$$

Once this equation system is solved, the surface charge density separated across the ITIES can be evaluated as

$$Q \equiv -\int_{-\infty}^{0} \rho \mathrm{d}x = \frac{2\varepsilon_0 RT}{F}\left[\left(\kappa_{\mathrm{o}}^2\varepsilon_o^2 - \kappa_{\mathrm{hc}}^2\varepsilon_{\mathrm{hc}}^2\right)\sinh^2\frac{\varphi(-d_{\mathrm{hc}})}{2} + \kappa_{\mathrm{hc}}^2\varepsilon_{\mathrm{hc}}^2 \sinh^2\frac{\varphi(0)}{2}\right]^{1/2} \tag{7}$$

and the interfacial capacitance is calculated (by numerical differentiation) from Eq. (1); note that Eq. (7) was incorrectly written in Refs. [29] and [30], although the results obtained thereof are correct and not affected by this typographical error.

3. Experimental

3.1. Chemicals

The solvent of the organic phase was 1,2-dichloroethane (1,2-DCE, Aldrich, spectrophotometric grade). The aqueous base electrolyte was sodium chloride (NaCl, Merck, p.a.) and sodium tetraphenylborate (NaTPB, Aldrich, >99.5%). Tetraoctylammonium tetraphenylborate (TOATPB) was prepared by precipitation of equimolar water/methanol 1:1 solutions of tetraoctylammonium chloride (TOACl, from Fluka, >97%) and NaTPB and recrystallized with acetone. Lithium chloride (LiCl, Merck, p.a.) was used as aqueous phase solutions. All aqueous solutions were prepared using fresh Milli-Q treated water (resistivity $> 18\ \mathrm{M\Omega\ cm}$). All chemicals were used as received. All experiments were carried out at room temperature and at pH ~ 7.

DLPC (99%), DPPC (>99%), DSPC (99%), DAPC (99%), DBPC (>99%) were purchased from Sigma and used as received without further purification. The PCs were dissolved in chloroform and methanol. Then a stock solution was prepared dissolving the previous solution in an appropriate amount of 1,2-DCE. The PC solutions were prepared in nitrogen atmosphere and kept at a temperature of $-5\ ^\circ\mathrm{C}$.

3.2. Methods

Impedance measurements were carried out in a four-electrode cell with a flat 1,2-DCE/water interface of $0.28\ \mathrm{cm^2}$ as described elsewhere [31]. The electrochemical cell employed in this study is schematically represented by

$$\begin{aligned}&\mathrm{Ag|AgCl|10\ mM\ NaTPB}\\&\quad +\mathrm{10\ mM\ NaCl\ (H_2O)|10\ mM\ TOATPB}\\&\quad +x\ \mu\mathrm{M\ PC\ (1,2-DCE)|LiCl\ 100\ mM,\ pH}\sim 7\ \mathrm{(H_2O)|AgCl}\end{aligned}$$

where PC stands for DLPC, DPPC, DSPC, DAPC or DBPC, and x is the amount of phosphatidylcholine with concentrations from 0.1 to 100 μM.

Impedance spectra were measured with a frequency response analyser (1250 'Frequency Responde Analyser' Solartron, Solartron Instruments, UK) and a four-electrode potentiostat (1287 SI Solartron, Solartron Instruments, UK). In the equilibrium impedance measurements, a 0.020 V root-mean-square ac voltage from the FRA was applied, sweeping in the frequency range from 1 to 500 Hz with frequencies logarithmically spaced (15 points per decade). These impedance spectra were analysed using the equivalent circuit shown in Fig. 2 which is used to interpret the impedance data extracted from electrified liquid–liquid interfaces [32,33].

The capacitance was extracted and analysed from the impedance spectra by a non-linear least square fitting (EQUIVCRT software from Boukamp [34]), using as fitting parameters, R_s, C_d, and Z_w. Fitting errors were always less than 5%.

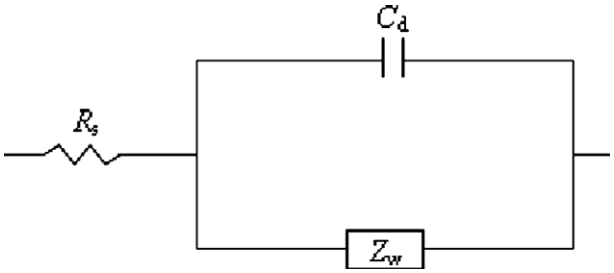

Fig. 2. Equivalent circuit where R_s is the solution resistance, C_d is the double layer capacitance and Z_w is the Warburg impedance.

The potential difference applied on the cell, V_{ap}, defined as the difference of aqueous phase reference electrode and the organic phase, was converted in a Galvani potential scale using a procedure described elsewhere [35] by using the cation tetraethylammonium as the reference ion probe ($\Delta\phi^{o'}_{w\to 1,2-DCE} = 0.019$ V) [36].

Impedance measurements were carried out 1 h after cell preparation. This stabilization time was found experimentally and was considered to be sufficient to reproducible adsorption of the phospholipid at the liquid–liquid interface. In order to ensure that undesired time effects are avoided the measuring program was carefully chosen. Briefly the impedance measuring program started at a potential where it is not expected a strong phospholipid adsorption and then scanned towards the more negative potential limit followed by a back scan towards the more positive potential limit and a third scan towards the initial potential. This potential programme insured that the initial and final potential measured was the same and therefore any disruption in the phospholipid layer should lead to major changes in the interfacial capacitance.

4. Results and discussion

The impedance spectra in the absence and in presence of phospholipid are plotted in Fig. 3. There is a net change in the Nyquist representation showing the effect of phospholipid on the electrochemical and structural properties of the interface. After the fitting of the data to the equivalent circuit represented in Fig. 2, the double layer capacitance for the ITIES can be extracted. As an example the fitting parameters used to analyse the experimental data displayed in Fig. 3 are presented in Table 1.

The variation of the double layer capacitance with the potential drop across the liquid–liquid interface is represented in Fig. 4a and b where the capacitance curves for the adsorption of different PCs at the 1,2-DCE/water interface at phospholipid concentrations of 2 and 20 μM, respectively. At more negative potentials the capacitance in the presence of phospholipid is lower than the base line which indicates the presence of an adsorbed layer [37], and

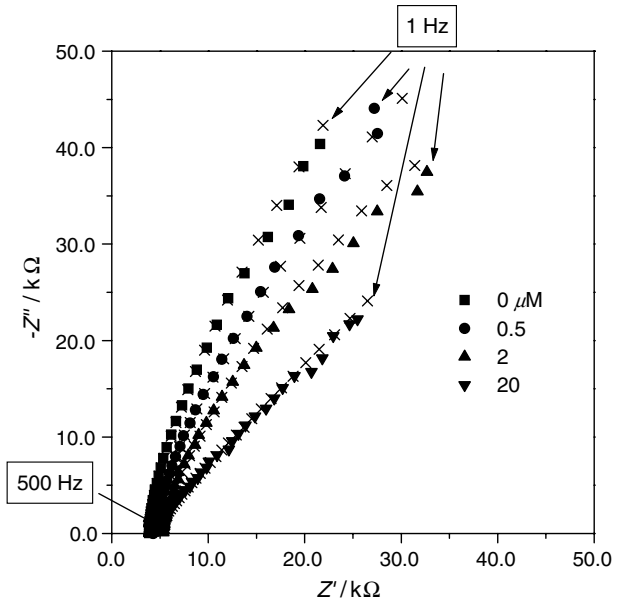

Fig. 3. Impedance spectra for the interface 1,2-DCE/water in the presence of different DLPC concentrations in the organic phase. $\Delta_o^w\phi = -0.100$ V. (×) Represents the fitting of the experimental data to the equivalent circuit shown in Fig. 2.

Table 1
Fitting parameter extracted from EQUIVCRT software for data displayed in Fig. 3

C_{lipid}/μM	R_s/Ω	Error/%	C/μF	Error/%	$Y_0 \times 10^6$	Error/%
0	3845	0.60	1.69	1.06	4.64	1.98
0.5	4375	0.50	1.07	0.84	5.18	0.94
2.0	4265	0.69	0.99	3.96	6.20	1.59
20.0	4677	1.11	0.32	3.27	11.23	0.98

where $\sigma = \frac{1}{\sqrt{2}Y_0}$.

decreases with increasing concentration until a constant value is reached which is usually taken as the formation of a saturated monolayer [12]. This is consistent with previous findings [28] in which the formation of a more compact layer also led to a lower curvature of the capacitance curves. The minimum of the capacitance curves observed at negative potentials suggests that the interface is positively charged [28,29]. This comes from an effective binding of the aqueous cations to the negative charge of the zwitterionic headgroups leading to a positive net charge. The minimum is slightly displaced to more positive potentials at increasing concentrations suggesting that the interface becomes less positively charged (probably due to the release of some cations because of the increasing vicinity of the headgroups).

At positive potentials the capacitance is strongly dependent on the chain length and two different trends are observed. For lower concentration and shorter chain length of the lipid the interfacial capacitance is generally higher or very close to the capacitance of the base line which is attributed by several authors to the interaction between the lipid and the cation in the aqueous phase [21]. For higher concentrations and for lipids with higher chain length ($n > 18$) the capacitance is lower than the base line, indicating the adsorption of the phospholipid in this potential region.

For higher concentrations and positive potentials it is clearly observed a trend of decreasing capacitance with increasing chain length (DAPC being the only exception). This behaviour does not hold at low concentrations because the interface is not compact and the capacitance depends on the system parameters in a more complicated way. The inclusion of ions from the organic phase is more significant in this latter case and this leads to more complex interactions. When the lipid concentration increases mobile ions tend to be more excluded from the hydrocarbon region possibly due to steric effects and the specific properties of each lipid (chain length being here the most important) play a more significant role.

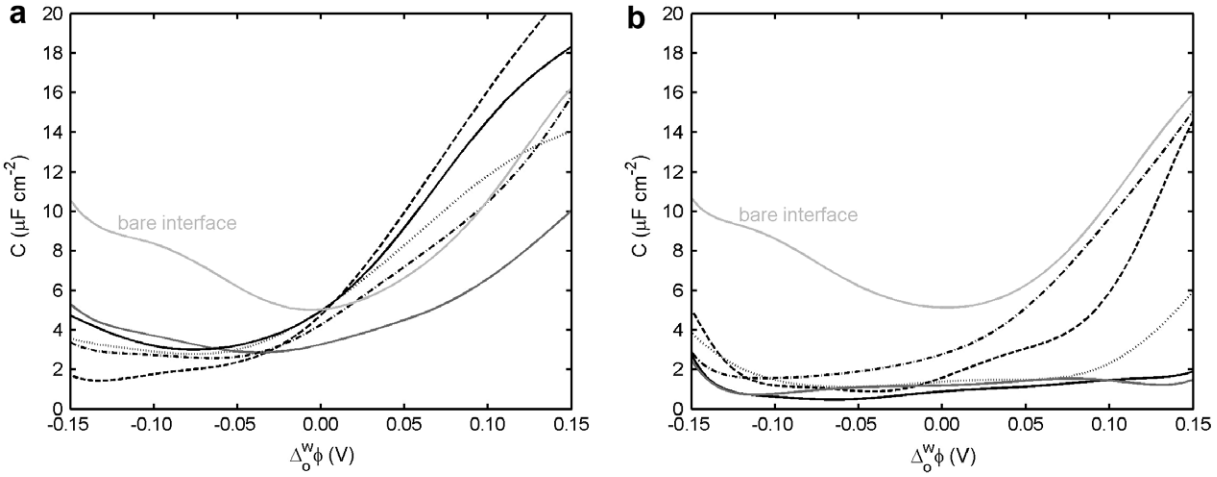

Fig. 4. Experimental capacitance curves for the following phospholipids deposited at the 1,2-DCE/water interface: DLPC (dash–dot line), DPPC (dashed line), DSPC (black continuous line), DAPC (dotted line) and DBPC (grey continuous line) and with concentrations 2 μM (a) and 20 μM (b). The capacitance curve of the bare interface is also shown.

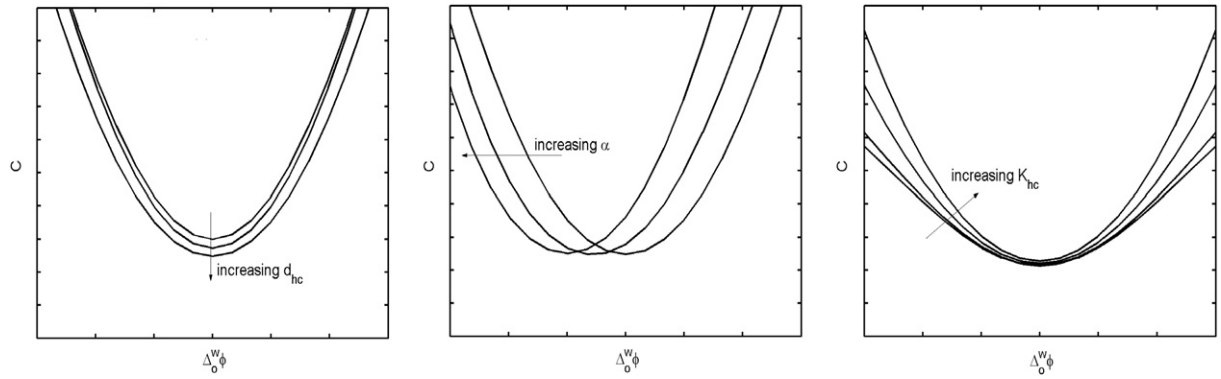

Fig. 5. Influence of the theoretical parameters on the capacitance curves.

All these observations can be satisfactorily explained and supported by means of our theoretical model which depends on three parameters: the thickness of the hydrocarbon region d_{hc}, the dimensionless surface charge density at the interface α, and the partition coefficient of the hydrocarbon region K_{hc}. The dependence of the interfacial capacitance on each theoretical parameter is depicted in Fig. 5. The parameter d_{hc} affect the capacitance values, as it could be expected from the expression of the geometrical capacitance of this layer, $C_{geom} = A\varepsilon_0\varepsilon_{hc}/d_{hc}$. An increase in this parameter leads to a decrease of the overall capacitance [28]. The dimensionless surface charge density α shifts horizontally the capacitance curves. Positive α values displace the capacitance minimum to negative potentials and the contrary holds for negative α. Finally, the curvature of the capacitance curves increases with increasing the partition coefficient K_{hc}. The theoretical values used are given in Table 2 for all phospholipids considered. Values for other theoretical parameters are $\varepsilon_o = 10.4$, $\varepsilon_w = 78.54$ and $\varepsilon_{hc} = 3$.

Table 2
Parameter values used in the calculations of capacitance curves for the different phospholipids

Phospholipid	d_{hc} (Å)	2 μM		20 μM	
		K_{hc}	α	K_{hc}	α
DLPC	10	0.02	0.17	0.015	0.17
DPPC	16	0.05	0.30	0.05	0.10
DSPC	19	0.14	0.15	0.0005	0.03
DAPC	22	0.07	0.11	0.02	0.07
DBPC	25	0.05	0.03	0.001	0.03

Fig. 6a and b shows the theoretical capacitance curves at lipid concentrations of 2 μM (a) and 20 μM (b). All the main features of the experimental curves are correctly reproduced qualitatively. The decrease of the capacitance with lipid concentration below the base line is explained through the decrease in the partition coefficient of the hydrocarbon region K_{hc} which leads to a lower curvature for the capacitance curves at higher lipid concentration. In Table 2, it can be observed that K_{hc} is generally lower at higher concentrations for a given lipid. This means that ions coming from the organic phase are excluded from the interfacial lipid layer (most probably due to steric effects:

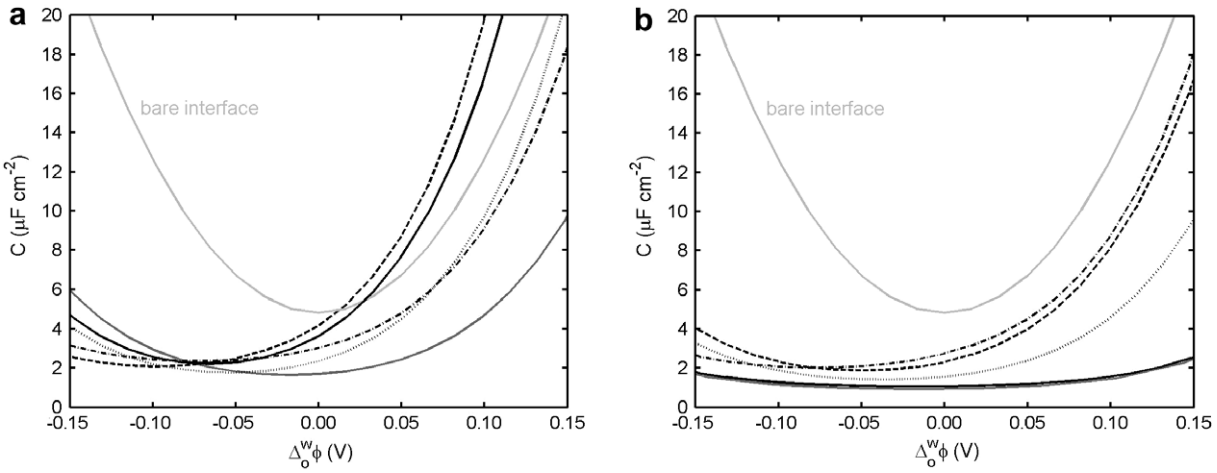

Fig. 6. Calculated capacitance curves for the following phospholipids deposited at the 1,2-DCE/water interface: DLPC (dash–dot line), DPPC (dashed line), DSPC (black continuous line), DAPC (dotted line) and DBPC (grey continuous line) and with concentrations 2 μM (a) and 20 μM (b). The capacitance curve of the bare interface is also shown.

the hydrocarbon region is now more compact because of the increased lipid concentration). At high lipid concentration (Fig. 6b) d_{hc} is proportional to the chain length of the lipids, and the decrease of the overall capacitance with increasing chain length is correctly reproduced by the theory. At low lipid concentration the hydrocarbon region is looser and d_{hc} is rather an effective parameter not necessarily proportional to the chain length.

At negative potentials the position of the capacitance minima is correctly reproduced through the surface charge density α which is positive for all lipids indicating the binding of the aqueous cations to the zwitterionic headgroups thus confirming the experimental observation made above. The slight displacement of the minimum to more positive potentials at higher lipid concentrations (Fig. 6b compared to 6a) is also explained through the generally lower value of α. At these concentrations, the zwiterionic headgroups are closer and this tends to preclude slightly the adsorption of the aqueous cations: the distance between sites for adsorption is lower as well as that of the same-charges that would be adsorbed. Steric effects can also play an important role since it is reasonable that the size of the adsorption sites will be lower for a more compact structure. As a result of all these factors, the interface will contain a lower concentration of aqueous cations and this explains the lower value of α which represents the net surface charge density at the interface. Another possible reason is a reorientation of the lipid headgroups allowing Cl^- ions to enter the interface thus lowering the net excess charge (and therefore, the value of α).

In Fig. 7, the electric potential distribution calculated from Eqs. (2)–(6) is represented for DAPC (parameters taken from Table 2) and from dimensionless potential drops $\Delta\varphi_o^w = \varphi_w^b - \varphi_o^b$ ranging from −3 to 3. The potential profile within the hydrocarbon region is almost linear and, although continuous at the interface, it reaches a peak leading to a discontinuity of the electric field. This is due to the net surface charge α at the interface.

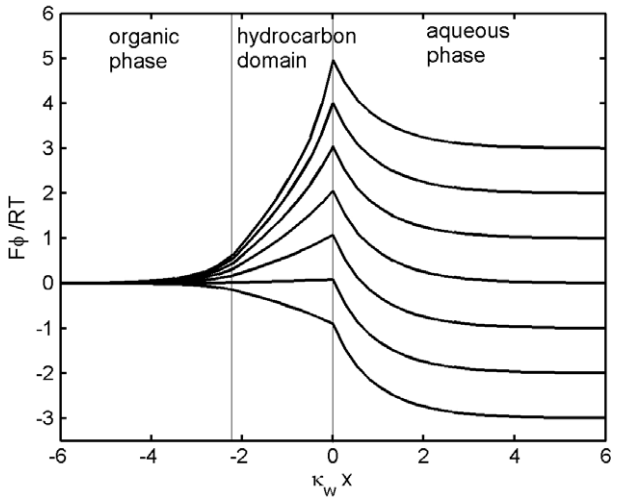

Fig. 7. Calculated potential distribution for DAPC at dimensionless potential drops $\Delta\varphi_o^w$: 3, 2, 1, 0, −1, −2, − 3 from top to bottom and parameter values given in Table 2.

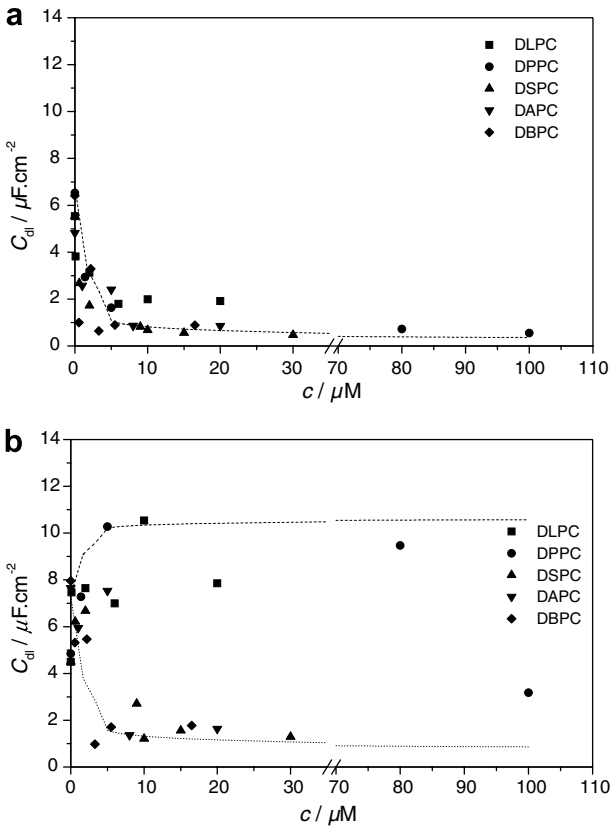

Fig. 8. Interfacial capacitance as a function of the lipid concentration measured at −0.070 V (a) and +0.070 V (b).

Fig. 8a and b shows the plot of the interfacial capacitance, for the different phospholipids as a function of the lipid concentration. Although there is a strong effect of the nature of the phospholipid in an intermediate concentration region (between 0.5 and 3 μM), there is a decrease in capacitance with the increase in concentration. A constant value for the saturated monolayers is obtained for all lipids when the concentrations are higher than 5 μM.

From Fig. 8a and b, it is possible to conclude that at negative potentials (−0.070 V) there is a decrease in the interfacial capacitance with the increase in phospholipid concentration. The dotted lines where added in order to show the trend of the measured capacitance with the increase in lipid concentration. For phospholipid concentrations higher than 5 μM saturation is reached which is generally interpreted as the formation of a saturated phase.

The behaviour of capacitance with lipid concentration is not linear and for some intermediate concentrations there is no clear trend, which probably reflects the different adsorption behaviour of the different lipids and could also be related with the adsorption kinetics. It should be stressed that for the intermediate concentrations, where the deviation from the linear trend was higher, three replicate measurements were made and no significant deviation was observed.

Adsorption of phospholipids has been interpreted by Kakiuchi and co-workers using the Frumkin isotherm, with weak lateral interactions. Adsorption of non-ionic surfactants has been treated with a simple model [16]:

$$\theta = \frac{C_D - C_D^{\theta=0}}{C_D^{\theta=1} - C_D^{\theta=0}} \quad (8)$$

where $C_D^{\theta=1}$ is the capacitance value at maximum coverage, $C_D^{\theta=0}$ is the capacitance value in the absence of surfactant, and θ is the fractional coverage of the surface. The model applies if the electrical potential is uniform over the surface (i.e., the patches are at least large enough that there are no discreteness-of-charge effects), and the surface coverage does not vary with perturbation of the interfacial potential difference used for the measurement.

The surface coverage θ was calculated using Eq. (8) for the minimum potential, and in the case of DSPC, DBPC and DAPC, a positive potential was also used for the calculation of the surface coverage. To analyse the results in Fig. 8, θ was fitted to the Frumkin adsorption isotherm [16]:

$$\beta c = \frac{\theta}{1-\theta} e^{-2a\theta} \quad (9)$$

where β is the adsorption equilibrium constant, c is the lipid concentration, and a is the lateral interaction parameter. Since $\ln\beta$ is equal to $-\Delta G^{o}_{ads}/RT$, the Gibbs energy of adsorption ΔG^{o}_{ads} can also be extracted from Eq. (9).

The fitting parameters were determined from plots of $\ln\{\theta/[C_{lipid} * (1-\theta)]\}$ vs. θ (resulting from the linearization of Eq. (9), results shown in Fig. 9a and b), with slope of $2a$ and abscissas interception of $\ln\beta$ and are summarize in Tables 3 and 4.

The results shown in Tables 3 and 4 can be interpreted as the existence of two distinct adsorption behaviours for the PCs under study. For PCs with chain length lower than C18 and for positive Galvani potentials, the capacitance curves no longer show the effect of lipid adsorption which was generally interpreted either as the change of orientation of the adsorbed molecules or the partial desorption of the lipid molecules [11]. Although for DSPC there is still adsorption at the interface the Gibbs energy of adsorption decreases relatively to the adsorption at negative potentials. For DAPC and DBPC there is no significant change in the Gibbs energy of adsorption with the potential difference across the interface. We should stress that the values of the interaction parameter of the Frumkin isotherm (a) are positive and large, particularly for DSPC, DAPC and DBPC for which they are close or above 2. According to Markin and Volkov [38] the expanded-condensed transition occurs when $a \geqslant 2$. The decrease in capacity reported in Fig. 4, at more positive potentials seems also to indicate that the adsorbed layer is in condensed phase.

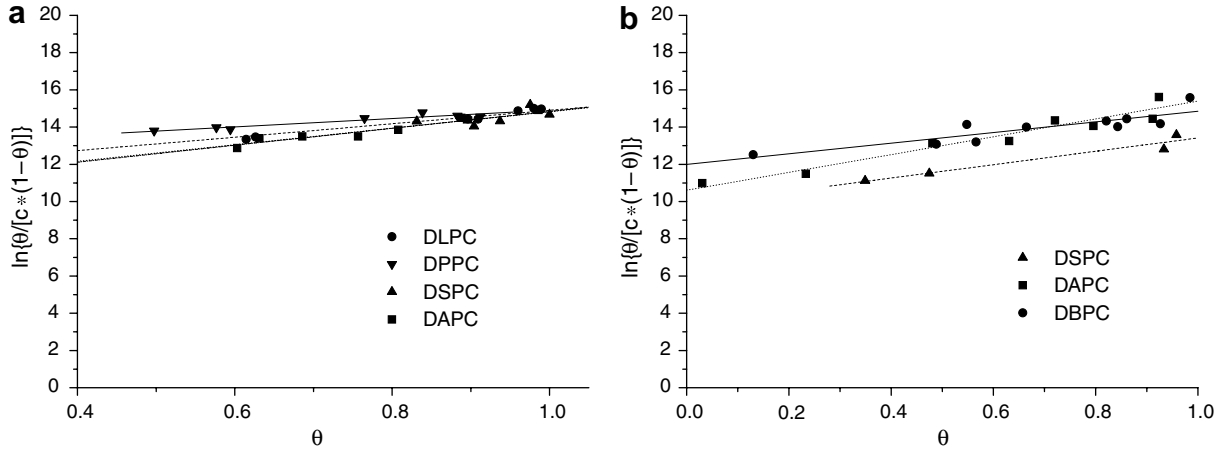

Fig. 9. Plot of $\ln\{\theta/[C_{lipid} * (1-\theta)]\}$ as a function of θ for the different phospholipids used in this study measured at −0.070 V (a) and +0.070 V (b).

Table 3
Experimental conditions and the extracted parameters from the non-linear fitting of experimental data to the Frumkin isotherm at negative Galvani potential

	DLPC	DPPC	DPPC[a]	DSPC	DAPC	DBPC
$\Delta\phi_{min.\ cap.}$/V	−0.110	−0.100	−0.125	−0.090	−0.070	−0.080
$C_D^{\theta=0}$/μF cm^{-2}	7.3	6.9	9.4	5.5	4.6	4.4
$C_D^{\theta=1}$/μF cm^{-2}	1.80	1.10	1.00	0.50	0.82	0.80
a	1.8	1.1	1.1	2.3	2.2	1.9
$\ln\beta$	11.3	11.9	13.4	10.3	10.5	11.4
ΔG^{o}_{ads}/kJ mol^{-1}	−28	−29	−33	−26	−26	−28

[a] In phosphate buffer.

Table 4
Experimental conditions and the extracted parameters from the non-linear fitting of experimental data to the Frumkin isotherm at positive Galvani potential

	DSPC	DAPC	DBPC
$\Delta\phi_{\text{min. cap.}}$/V	0.080	0.050	0.119
$C_D^{\theta=0}$/μF cm^{-2}	6.80	5.88	10.8
$C_D^{\theta=1}$/μF cm^{-2}	1.50	1.08	1.57
a	1.8	2.4	1.6
$\ln\beta$	9.8	10.6	12.5
ΔG^{o}_{ads}/kJ mol^{-1}	−24	−26	−31

5. Conclusions

The adsorption of PCs with chains of different length at the 1,2-DCE/water interface has been studied by measuring the interfacial capacitance at different potential ranges. A theoretical model based on the Poisson–Boltzmann equation has provided a successful explanation of all experimental trends observed for the dependence of phospholipid adsorption at the interface on the applied potential, lipid concentration and chain length. The dependence on chain length is most easily understood at high lipid concentrations in which larger chain lengths lead to higher thickness of the lipid layer and, therefore, lower overall capacitances. The higher the lipid concentration the lower the available space for the mobile ions at the hydrocarbon layer (because the structure is more compact). This is also correctly accounted for by means of a lower partition coefficient to the hydrocarbon region and it is evidenced by the decreasing curvature of the capacitance curves below the base line. For PCs with $n < 18$ it was observed, moreover an almost complete desorption from the interface, while for PCs with $n > 18$ no significant change in the Gibbs energy of adsorption for the potential range studied were observed.

Acknowledgements

Financial support from FCT for the project PRAXIS XXI/QUI/474 and from European Union under the research and training network SUSANA (“Supramolecular Self-Assembly of Interfacial Nanostructures”, Contract number HPRN-CT-2002-00185) is greatly acknowledged.

References

[1] B.Y. Yue, C.M. Jackson, J.A.G. Taylor, J. Mingins, B.A. Pethica, J. Chem. Soc., Faraday Trans. 1 72 (1976) 2685.
[2] J. Taylor, J. Mingins, B. Pethica, J. Chem. Soc., Faraday Trans. 1 72 (1976) 2694.
[3] M.C. Phillips, D. Chapman, Biochim. Biophys. Acta 163 (1968) 301.
[4] J. Mingins, J.A.G. Taylor, B.A. Pethica, C.M. Jackson, B.Y.T. Yue, J. Chem. Soc., Faraday Tans. 1 78 (1982) 323.
[5] R.A. Walker, J.C. Conboy, G.L. Richmond, Langmuir 13 (1997) 3070.
[6] D. Grandell, L. Murtomäki, K. Kontturi, G. Sundholm, J. Electroanal. Chem. 463 (1999) 242.
[7] H. Matsumura, K. Furusawa, Adv. Coll. Interf. Sci. 30 (1989) 71.
[8] A. Watanabe, M. Matsumoto, H. Tamai, R. Gotoh, Kolloid Z. Z. Polym. 228 (1968) 58.
[9] A. Watanabe, A. Fujii, Y. Sakamori, K. Higashituji, H. Tamai, Kolloid Z. Z. Polym. 243 (1971) 42.
[10] H.H. Girault, D.J. Schiffrin, J. Electroanal. Chem. 179 (1984) 277.
[11] T. Kakiuchi, M. Yamane, T. Osakai, M. Senda, Bull. Chem. Soc. Jpn. 60 (1987) 4223.
[12] T. Kakiuchi, M. Kotani, J. Noguchi, M. Nakanishi, M. Senda, J. Coll. Interf. Sci. 49 (1992) 279.
[13] T. Kakiuchi, T. Kondo, M. Kotani, M. Senda, Langmuir 8 (1992) 169.
[14] T. Kakiuchi, T. Kondo, M. Senda, Bull. Chem. Soc. Jpn. 63 (1990) 3270.
[15] T. Kakiuchi, M. Nakanishi, M. Senda, Bull. Chem. Soc. Jpn. 61 (1988) 1845.
[16] T. Kakiuchi, M. Nakanishi, M. Senda, Bull. Chem. Soc. Jpn. 62 (1989) 403.
[17] T. Wandlowski, S. Racinsky, V. Mareček, Z. Samec, J. Electroanal. Chem. 227 (1987) 281.
[18] T. Wandlowski, V. Mareček, Z. Samec, J. Electroanal. Chem. 242 (1988) 277.
[19] S.G. Chesniuk, S.A. Dassie, L.M. Yudi, A.M. Baruzzi, Electrochim. Acta 43 (1998) 2175.
[20] Y. Yoshida, H. Yoshinaga, N. Ichieda, A. Uehara, M. Kasuno, K. Banu, K. Maeda, S. Kihara, Anal. Sci. 17 (2001) i1037.
[21] Z. Samec, A. Trojánek, H.H. Girault, Electrochem. Commun. 5 (2003) 98.
[22] D. Grandell, L. Murtomäki, Langmuir 14 (1998) 556.
[23] V. Rosilio, M.-M. Boissonade, J. Zhang, L. Jiang, A. Baszkin, Langmuir 13 (1997) 4669.
[24] A. Miller, H.J. Möhwald, J. Chem. Phys. 86 (1987) 4258.
[25] P. Liljeroth, A. Mälkiä, V.J. Cunnane, A.-K. Kontturi, K. Kontturi, Langmuir 16 (2000) 6667.
[26] A. Mälkiä, P. Liljeroth, A.-K. Kontturi, K. Kontturi, J. Phys. Chem. B 105 (2001) 10884.
[27] A. Mälkiä, P. Liljeroth, K. Kontturi, Anal. Sci. 17 (2001) i345.
[28] H.A. Santos, V. García-Morales, R.-J. Roozeman, J.A. Manzanares, K. Kontturi, Langmuir 21 (2005) 5475.
[29] H.A. Santos, M. Chirea, V. García-Morales, F. Silva, J.A. Manzanares, K. Kontturi, J. Phys. Chem. B 109 (2005) 20105.
[30] C.J. Slevin, A. Mälkiä, P. Liljeroth, M. Toiminen, K. Kontturi, Langmuir 19 (2003) 1287.
[31] C.M. Pereira, W. Schmickler, F. Silva, M.J. Sousa, J. Electroanal. Chem. 436 (1997) 9.
[32] Z. Samec, A. Trojánek, J. Langmaier, J. Electroanal. Chem. 444 (1998) 1.
[33] C.M. Pereira, F. Silva, M.J. Sousa, K. Kontturi, L. Murtomäki, J. Electroanal. Chem. 509 (2001) 48.
[34] B.A. Boukamp, Solid State Ionics 18–19 (1986) 136.
[35] A.J. Blake, M.H.M. Caçote, F.A. Devillanova, A. Garau, F. Isaia, V. Lippolis, C.M. Pereira, F. Silva, L. Tei, Eur. J. Inorg. Chem. (2002) 1816.
[36] T. Wandlowski, V. Mareček, Z. Samec, Electrochim. Acta 35 (1990) 1173.
[37] D. Bizzotto, V. Zamlynny, I. Burgess, C.A. Jeffrey, H.-Q. Li, J. Rubinstein, R.A. Merril, J. Lipkowski, Z. Galus, A. Nelson, B. Pettinger, Amphiphilic and ionic surfactant at electrified interfaces, in: A. Wieckowski (Ed.), Interfacial Electrochemistry, Marcel Dekker, NY, 1999, pp. 405–426.
[38] V.S. Markin, A.G. Volkov, Adsorption isotherms and the structure of oil/water interfaces, in: A.G. Volkov, D.W. Deamer (Eds.), Liquid–Liquid Interfaces: Theory and Methods, CRC Press, Boca Raton, Florida, 1996.